Timing of lake-level changes for a deep last-glacial Lake Missoula: optical dating of the Garden Gulch area, Montana, USA

Smith, Larry N.; Sohbati, Reza; Buylaert, Jan-Pieter; Lian, Olav B.; Murray, Andrew Sean; Jain, Mayank

Published in:
Quaternary Science Reviews

Link to article, DOI:
10.1016/j.quascirev.2018.01.009

Publication date:
2018

Document Version
Peer reviewed version

Timing of lake-level changes for a deep last-glacial Lake Missoula: optical dating of the Garden Gulch area, Montana, USA

Larry N. Smith[1*], Reza Sohbati[2], Jan-Pieter Buylaret[2, 3], Olav B. Lian[4], Andrew Murray[2,3], and Mayank Jain[2]

[1] Department of Geological Engineering, Montana Tech of the University of Montana, 1300 W. Park St., Butte, MT 59701, United States

[2] Center for Nuclear Technologies, Technical University of Denmark, DTU Risø Campus, Roskilde 4000, Denmark

[3]Nordic Laboratory for Luminescence Dating, Aarhus University, DTU Risø Campus, Roskilde 4000, Denmark

[4]Department of Geography and the Environment, University of the Fraser Valley, Abbotsford, British Columbia, V2S 7M8, Canada

** Corresponding author, lsmith@mtech.edu*

Abstract

Glaciolacustrine sediments in the Clark Fork River valley at Garden Gulch, near Drummond, Montana, USA record highstand positions of the ice-dammed glacial Lake Missoula and repeated subaerial exposure. During these highstands the lake was at greater than 65% of its recognized maximum capacity. The initial lake transgression deposited a basal sand unit. Subsequent cycles of lake-level fluctuations are recorded by sequences of laminated and cross laminated silt, sand, and clay deformed by periglacial processes during intervening periods of lower lake levels.

Optically stimulated luminescence (OSL) dating of quartz sand grains, using single-aliquot regenerative-dose procedures, was carried out on 17 samples. Comparison of infrared stimulated luminescence (IRSL) from K-rich feldspar to OSL from quartz for all the samples suggests that they were well bleached prior to deposition and burial. Ages for the basal sand and overlying glaciolacustrine exposure surfaces are indistinguishable within one standard deviation, and give a weighted mean age of 20.9 ± 1.3 ka (n=11). Based on sedimentological and stratigraphic analysis we infer that the initial transgression, and at least six cycles of lake-level fluctuation, occurred over time scales of decades to ~2 ka. Bioturbated sandy slopewash dated at 10.6 ± 0.9 ka and 11.9 ± 1.2 ka unconformably overlies the upper glaciolacustrine deposits. The uppermost sediments, above the glaciolacustrine section, are younger than the Glacier Peak tephra (13.7-13.4 cal. ka B.P.), which was deposited across parts of the drained lake basin, but has not been found at Garden Gulch.

Our study indicates that glacial Lake Missoula reached >65 percent of maximum capacity by about 20.9 ± 1.3 ka and either partially or completely drained twelve times from this position. Rapid lowering from the lake's highstand position due to ice-dam failure likely led to scour in

the downstream portions of the glacial Lake Missoula basin and megafloods in the Channeled Scabland.

HIGHLIGHTS

- Glacial Lake Missoula rose and fell near its full-pool volume at 20.9 ± 1.3 ka (n=11)
- Post-lake sediment ages (n=3) support cessation of lake sedimentation by 13.7-13.4 ka
- Garden Gulch geochronology is consistent with early Channeled Scabland megafloods

KEYWORDS

Quaternary; North America; glacial Lake Missoula; Optical dating methods; Periglacial

1. Introduction

Glacial Lake Missoula was an ice-dammed lake that inundated about 9,500 km^2 of the intermontane valleys of western Montana during the latest Pleistocene glaciation (Breckenridge et al., 1989; Pardee, 1910, 1942). Rapid emptying of glacial Lake Missoula caused giant late Pleistocene floods, or megafloods, that carved the Channeled Scabland of Washington State. The age of glacial Lake Missoula and its lake-level history is primarily inferred from the chronology of downstream flooding in the Channeled Scabland (Atwater, 1987, 1984; Baker and Bunker, 1985; Balbas et al., 2017; Clague et al., 2003; O'Connor and Baker, 1992; Waitt, 1980, 1985; Waitt et al., 2009), the Columbia River Gorge (Benito and O'Connor, 2003), and recorded in offshore deposits in the eastern Pacific Ocean (Gombiner et al., 2016; Zuffa et al., 2000). Recognition of multiple floods in the downstream areas led these workers to propose various combinations of one or many more complete or partial drainings during the latest Pleistocene glaciation (~21 to 14 cal. ka B.P.[1]) (Breckenridge and Phillips, 2010; Carrara et al., 1996; Clague et al., 2003; Hanson and Clague, 2016; Smith and Hanson, 2014; Waitt, 1985, 1980). Therefore

[1] All radiocarbon ages are reported as cal. ka B.P. or cal. yr B.P., depending on how they were originally published, and were calibrated with OxCal 4.2 using the IntCal13 calibration curve (Reimer et al., 2013). Optical ages are reported in ka with standard error.

these multiple filling and draining cycles should have created a complex set of deposits within the basin concurrent with downstream flood deposits. Direct dating of the glacial Lake Missoula deposits in outcrop has been hindered by the absence of fossils, organic carbon, and volcanic tephra.

Dating of the lake deposits provides information complementary to the flood history as inferred from downstream deposits. Although obvious evidence for the lake and for highstand altitudes are wave-cut shorelines (Pardee, 1910), they are discontinuous erosional features and difficult to date. They reach altitudes of 1260-1298 m asl in the Missoula area (Pardee, 1910). Because post-glacial isostatic adjustment has not been estimated from the locally preserved shorelines, a 1280 m altitude maximum highstand is generally accepted (Alho et al., 2010; Pardee, 1910). Lake-bottom sediments are preserved along valley floors in the lake basin from near the former ice dam (at an altitude of 630 m) to ~100 m below the lake highstand of about 1280 m. So far, dating of glacial Lake Missoula has relied on optically stimulated luminescence (OSL or optical dating) analysis of glaciolacustrine deposits (Hanson et al., 2012). Optical dating gives an estimate of the time elapsed since quartz and feldspar grains were last exposed to sunlight, which usually dates deposition and burial; it has proven to be a powerful technique for dating sedimentary deposits (e.g. Roberts and Lian, 2015). Hanson et al. (2012) used optical dating of quartz on glaciolacustrine deposits at the Ninemile and Rail line sections (Fig. 1). Their age for alluvial sand below glaciolacustrine deposits at the Ninemile section was 15.1 ± 0.6 ka and ages for two horizons within glaciolacustrine deposits at the Rail line exposure were 14.8 ± 0.7 and 12.6 ± 0.6 ka (Hanson et al., 2012). A pine needle recovered from near the top of lake deposits, but below the Glacier Peak G tephra, in a core from Flathead Lake, ~100 km north of the Ninemile and Rail line sites (Fig. 1), gave a radiocarbon age of 12,330 ± 50 yr BP (Beta-

183416) (M.H. Hofmann pers. comm. 14 February 2017), or 14327 - 13965 cal yr B.P. (at two sigma), which was reported as 14,150 ± 50 cal yr BP by Hofmann and Hendrix (2010). These previous published ages were for sediments deposited below 980 m altitudes, which may represent <20% of the full-pool volume of the lake (Fig. 1). The development of a full history of lake-lowering and lake-filling cycles of sedimentation requires dating deposits at multiple altitudes in the lake basin.

The purpose of the present work is to propose a glacial Lake Missoula history from the Garden Gulch area along the Clark Fork River, Montana. These outcrops are topographically higher than those previously dated and therefore may record water-level fluctuations of deeper lake stands. We present optical ages on alluvium and periglacially modified surfaces of subaerial exposures in three glaciolacustrine sections.

2. Stratigraphic and geomorphic setting

Glaciolacustrine silt and clay of the former lake bottom locally blanket the Clark Fork River and Flathead River valleys (Figs. 1, 2). Glaciolacustrine sediments near Garden Gulch along the Clark Fork River, about 10 km northwest of Drummond, Montana, are among the highest elevation deposits recognized in the lake basin (Berg, 2005, 2006, Lonn et al., 2007, 2010). The site is 75 km upstream of the Missoula and Ninemile valleys and 350 km upstream of the Purcell Trench ice dam, at altitudes of 1173–1186 m. The deposits were excavated to depths of >13 m across a meander loop of the Clark Fork River (Figs. 1, 2). This excavation occurred during straightening of the railbed between 1883 and 1915 (Campbell et al., 1915). The deposits were apparently not eroded due to protection by a bedrock outcrop along the upstream (eastern) margin. The sediments record lake levels above elevations of ~1200 m and water volumes of ≥65 percent of the maximum recognized size of glacial Lake Missoula (Fig. 1). The location,

sedimentology, and periglacial features of two of the three measured sections (Fig. 3, sections I and II) at the site were described previously (Smith, 2017; Smith and Hanson, 2014).

Stratigraphic sections were measured along the top of the talus using standard field techniques (Figs. 3, 4). Section II is a composite of eight sections correlated by distinctive beds (Smith, 2017). The other sections were measured in continuous excavations. Loose, dried sediment was removed to depths of 0.2–1 m in 1–4 m-wide vertical swaths along the outcrop and then the exposed section faces were scraped with sharpened tools. The exposed deposits in the Garden Gulch area include, from the bottom to top, (1) a fining-upward sequence of paleo-Clark Fork River alluvium over bedrock; (2) transgressive basal sand; (3) rhythmically bedded glaciolacustrine deposits, and (4) capping slopewash with pedogenic alteration (Fig. 3). These units are described in detail in the following.

2.1 Paleo-Clark Fork alluvium

The lower portion of two outcrops at sections I and II (Fig. 3) are cobble and boulder-sized gravel with a coarse-grained sand matrix with west-directed (downstream) paleocurrent indicators. These deposits are interpreted as alluvium deposited by the Clark Fork River prior to inundation by glacial Lake Missoula (Smith, 2017). The gravel is overlain by locally derived colluvium and alluvium at section I, which is cross cut by medium-grained fluvial sand that overlies gravel at section II.

2.2 Deposits of the glacial Lake Missoula transgression (basal sand)

Sand with minor gravel was deposited across an inclined surface near section I and over paleo-Clark Fork River alluvium at section II. The unit ranges in thickness from about 5–100 cm. It contains moderately sorted cross-stratified sand and poorly sorted sandy angular and subangular gravel of locally derived Jurassic and Cretaceous sedimentary rocks (Fig. 2). At the

top of the sandy gravel, rhythmically laminated beds of coarse and medium-grained silt are interbedded with gravelly sand, and intraclasts of laminated glaciolacustrine sediment; these fragments indicate that dried or frozen lake-bottom sediments were incorporated into the basal sand (Figs. 4B, C). Interlayering of this unit with overlying glaciolacustrine sediment indicates deposition during a transition from fluvial to glaciolacustrine sedimentation as glacial Lake Missoula transgressed eastward to this location (Smith, 2017). At section III the transgressive deposits consist of 3-5 cm of silty sand with minor gravel deposited over fractured bedrock (Fig. 3).

2.3 Periglacially modified glaciolacustrine deposits and silty gravel

Most of the exposure shown in Figure 4 is made up of cycles of rhythmically bedded glaciolacustrine silt and clay with intervening beds of silty gravel. Each of the 12 sequences shown in Figure 3, section II, contains glaciolacustrine deposits of glacial Lake Missoula that fine-upward from ripple-cross laminated very fine- to fine-grained silty sand to rhythmically bedded silt, and less common clay, couplets. All but the upper two cycles, "*k*" and "*l*", are capped by silty gravel deposits that are then overlain by the basal sand or silt of the overlying fining-upward sequence. The number of rhythmically laminated couplets in the 12 glaciolacustrine cyclic sequences range from >7 to >110; however, interpreting these as varves is speculative (Smith, 2017). The uppermost sequence of laminated glaciolacustrine sediment (Fig. 3, section II "*l*") transitions upward to fine-grained sand due to being mixed by meniscate burrows that extend downward from the overlying deposit.

The upper portions of the lower 11 cycles ("*a*" to "*k*") are characteristically deformed by cracks, minor faults, and upturned and downturned deformational structures, with locally homogenized bedding (Fig. 3, section II; Figs. 4E, F). Downward-tapering wedges at the tops of

cycles "*a*" to "*j*" are filled by gravel, silt, and sand separated by massive silt and clay with locally preserved laminations. Gravel clasts are angular, fine-grained and metamorphosed siltstone and sandstone identical to those found in nearby outcrops of Jurassic-Cretaceous sandstone and siltstone (Fig. 3). Gravel clasts have vertical orientations and other features characteristic of cryoturbation (Smith, 2017).

The deformational features at the tops of each of the 12 cycles represent subaerial exposure of glacial Lake Missoula sediment during drops in lake level. Transport of the locally derived, angular gravel onto an exposed lake floor is interpreted to have been by entrainment of hillslope debris during water-level lowering, as more completely described in Smith (2017). The sediment-filled wedges and deformed bedding in the silty sediment horizons are interpreted as seasonal frost cracks and active-layer deformation features that formed in seasonally cold climate. Arkosic sand mixed with the gravel at the tops of cycles "*a*" to "*f*" was derived from granitic terrain upstream of the site and became mixed with the gravel by cryoturbation. The abrupt contacts where disturbed bedding is overlain by laminated light gray silt or very fine-grained sand, such as at the top of cycles "*b*" and "*c*" (Fig. 4E, F), show that subaerial exposure surfaces were buried during the next glacial-lake transgression, representing reestablishment of glacial Lake Missoula. The final retreat of glacial Lake Missoula from this site was marked by bioturbation of glaciolacustrine deposits near the top of cycle "*l*".

2.4 Post-lake sediment

Rhythmically laminated glaciolacustrine sediments are overlain by massive bioturbated sandy silt, silty sand, and intraclast conglomerate, between 0.7 to >2 m in thickness along the outcrop (Figs. 3, 4G). Burrowing at the lower contact of the post-lake sediment continues downward into laminated glaciolacustrine silt and clay (Fig. 3, section II; Fig. 4G). Massive

bedding, carbonate nodules, and carbonized rootlets suggest weak pedogenic modification of the silty unit, which likely includes reworked glaciolacustrine sediment. Brecciation and erosion of the uppermost portion is attributed to human excavation for realignment of the Clark Fork River.

3. Sampling for optical dating

Sedimentary units with visible sand-sized quartz grains were selected for sampling for optical dating. Sampling was done in the field by pounding 25 to 30-cm long, 4-cm internal diameter opaque aluminum or plastic tubes into the outcrop (making sure to pack the sediment tightly to avoid mixing). Tubes were then excavated and tightly secured at the ends to preserve water content and prevent mixing during transport. Due to cm-scale layering in much of the strata, sediment within 30 cm of the tubes was also sampled during excavation for additional environmental dose-rate determinations.

A total number of 17 samples were collected for optical dating; four samples from the basal sand, 10 samples from the glaciolacustrine deposits and three samples from the bioturbated slopewash post-lake sediments near the top of section II (Fig. 3). The basal sand samples were collected from each of the exposed alluvial units directly below the glaciolacustrine sediment at sections I and II (Fig. 3). At section I the unit was sampled from alluvial cross-stratified sand (JD-01; Fig. 4B). The two samples in the fluvial sediments at section II were collected 10 and 66 cm below the glaciolacustrine sediments (167502 and 167521; Fig. 4A). The silty sand over bedrock sample at section III (167525; Fig. 3) included gravel-sized clasts from the underlying bedrock (Figs. 2, 3).

The glaciolacustrine samples were taken from seven stratigraphic positions. Sediment within eight downward-tapering wedges was sampled at six stratigraphic levels; one sample was from rippled silt within glaciolacustrine silt and clay (JD-02; Fig. 4A) and two from rippled sand

overlying periglacially modified silty gravel (167504, 167505; Fig. 3). Periglacial wedges at the tops of the upper six cycles contain little visually identifiable sand and were therefore not sampled. One sample (167520) is from a massive sand bed that overlies cycle *"a"*; the sand shows soft-sediment deformation structures where it intrudes, and contains pillows of overlying glaciolacustrine silt (Fig. 4D). We infer that this sand body was fluidized during a lake-level fall (Smith, 2017). One sample (JD-02) was taken from a 0.2 m-thick unit displaying climbing ripples about 65 cm above the base of the glaciolacustrine unit (Figs. 3, 4A).

The bioturbated sediment near the top of section II was sampled above and below a weakly developed soil horizon at the top of the glaciolacustrine section (Figure 4 G, H; 167511, 167512). An additional sample is from a massive silty unit at the highest stratigraphic level of exposure (Fig. 3; JD-03).

4. Sample preparation, instrumentation, and analysis

The samples were prepared and analyzed at two different laboratories, three at the Luminescence Dating Laboratory at University of Fraser Valley (UFV), British Columbia, Canada, and 14 at the Nordic Centre for Luminescence Research, DTU Risø Campus (NCLR); slight differences in procedures used at these laboratories are detailed below. Two samples processed at UFV are from equivalent stratigraphic horizons as those processed at NCLR in order to provide independent duplicate ages on these horizons.

All samples were prepared using standard procedures under laboratory darkroom conditions. The outer 5-7 cm of sediment was removed from each end of the tubes to avoid possible contamination with sediments exposed to light and for environmental dose-rate measurements. The interior sample was wet-sieved to 180-250 µm diameter grains and treated with 10% H_2O_2 (1 h) to remove any organics, and then with 10% HCl acid for at least 1 h to

remove carbonates. HCl treatments were completed to the point of no visible reaction. At NCLR the grains were pre-etched with 10% HF acid for 20 minutes. Heavy-liquid separation (2.58 g/cm^3) was used to separate quartz from K-rich feldspar. The quartz extracts were then etched for 1 h using 40% HF (40 min. with 48% HF at UFV) to remove any remaining feldspar contamination and the outer alpha-irradiated layer of the quartz grains. The grains were then treated with 10% HCl for at least 40 minutes and rinsed in deionized water to remove any fluoride precipitates. The absence of feldspar contamination was tested using infrared (IR) stimulation, through an OSL IR depletion test (Duller, 2003); samples that had OSL IR depletion ratios greater than 10% of unity were treated a second time with 40% HF at NCLR. The overall OSL IR depletion ratio was 0.97 ± 0.01 (n=254), indicating that any feldspar contamination of the quartz signals was negligible. No further treatment was done on K-rich fractions after separation. Insufficient fine to medium-grained quartz sand was recovered from sample JD-02 so this sample was abandoned.

Luminescence measurements were made using multiple Risø TL/OSL DA-20 readers. Quartz was stimulated using blue (470 ± 30 nm, ~80 mWcm^{-2}) LEDs and detected through a 7.5 mm-thick Hoya U-340 glass filter. K-feldspar was measured using IR stimulation (870 ± 40 nm, ~135 mW cm^{-2}) with photon detection through a combination of Schott BG39 and Corning 7-59 glass filters. Laboratory beta irradiations employed ^{90}Sr/^{90}Y beta sources mounted on the readers that delivered calibrated doses between 0.07 and 0.22 Gy per second of beta exposure to 180-250 µm grains mounted on holders using silicon oil (Silkospray) fixing agent. Loose grains were removed from holders before measurement. At UFV, aluminum disks were used for small aliquots containing 50-100 grains. Stainless steel cups were used at NCLR for large aliquots (~8 mm) containing hundreds of grains.

The single-aliquot regenerative-dose (SAR) procedure was used for both quartz (Wintle and Murray, 2006) and feldspar (Wallinga et al., 2000) measurements. Quartz aliquots were stimulated at 125°C for 40 s. At NCLR signals for quartz were derived using an early background subtraction (signal: 0–0.32 s; background: 0.32–1.12 s) to isolate the fast components of the luminescence signal (e.g. Cunningham and Wallinga, 2010). Measurements made at UFV used the late background subtraction technique (signal 0–0.4 s; background 80–100 s). K-feldspar fractions were measured at 50°C with a thermal treatment (preheat) of 250°C for 60 s following both the regenerative and test doses. Aliquots were accepted or rejected on the basis of standard quality control tests (Wintle and Murray, 2006). Aliquots with D_e values greater than three standard deviations of the average for that sample were rejected as outliers.

5. Environmental dose rates

Environmental dose rates for samples analyzed at NCLR were found using high-resolution gamma spectroscopy (Murray et al., 1987). Each sample at NCLR included two dose rate measurements, one from the sample tube and one from sediment surrounding the tube. About 200 g (106-260 g) of sample from sample tube ends, or from the separate samples, were ashed (24 h at 450°C) and then ground and cast with melted wax in a fixed cup geometry. After 3 weeks of storage to let ^{222}Rn reach equilibrium with its parent ^{226}Ra, the cups were counted for 8 to >24 h using a gamma spectrometer. Dose rate samples run at UFV were calculated on sample splits using concentrations of ^{40}K, ^{238}U, and ^{232}Th found by neutron-activation analysis (NAA).

Pore water in the sediment matrix attenuates dose rate to mineral grains; therefore the average pore-water content of each sample needs to be estimated for dose-rate calculations. Sediment with natural moisture contents were collected in film canisters or from the sample

tubes. The as-collected (*in situ*) and saturated water contents of samples at both NCLR and UFV were measured by oven-drying at ~40°C.

The geomorphic position, approximate water-holding capacity, water-table history, and excavation history of the outcrops were considered in the estimation of the time-averaged water contents for samples. During deposition of lacustrine deposits the pores must have been saturated. After withdrawal of the lake and upon alluvial downcutting, the sediments were partially drained. The resulting time-averaged pore-water percentage depends on the sediment's water-holding capacity and its height above local base level, the Clark Fork River. Because all of the samples were taken from artificial excavations of a fluvial meander loop, *in-situ* water content measurements are considered too low, especially for those samples from the deepest part of the excavation. Average depths to the water table in thin (3–10 m) alluvial sediments along the Clark Fork River valley is about 3.8 m, but varies seasonally by about 3 m (Montana Bureau of Mines and Geology Ground Water Information Database data mbmggwic.mtech.edu). Therefore, water contents were estimated by averaging measured *in situ* values and saturated values for all but one near-surface sample (JD-03). An uncertainty of ±6% was ascribed to the water content values to account for uncertainty in these estimates.

Dose-rate conversion factors of Guérin et al. (2011), moisture content, and cosmic ray contributions based on present burial depths (Prescott and Hutton, 1994) were used to calculate environmental dose rates for all of the samples, and these are presented in Table 1.

6. Quartz luminescence characteristics

We first addressed the luminescence and dosimetry characteristics of the sampled quartz grains. A representative dose response curve and natural OSL decay curve for quartz extracted from sample 167501 is shown in Figure 5a together with the OSL curve from Risø calibration

quartz (Hansen et al., 2015). The similarity in luminescence responses shows that the OSL of the quartz samples is dominated by the desired thermally-stable fast component (Jain et al., 2003; Singarayer and Bailey, 2003).

To determine the appropriate preheat treatment, a preheat-plateau test was carried out on sample 167502 (Fig. 5b). The average value is shown as a dashed line and although the data are scattered, there is no apparent systematic dependence of equivalent dose (D_e) on preheat temperature in the range of 160 to 300 °C. A dose-recovery preheat-plateau test from 160 to 300 ºC of 167502 was undertaken by exposing 24 aliquots, respectively, to blue light at room temperature for 100 s, storing them for 10 ks, and then exposing them again to blue light to remove effects of thermal transfer, before giving them a dose that was then recovered (Wintle and Murray, 2000, 2006). Although there may be a weak systematic dependence of dose-recovery ratio on temperature, all results up to 280°C are within 10% of unity (Fig. 5c).

From these data, we adopted a preheat temperature of ≤ 260°C (with a cut-heat 40°C lower than preheat) for all D_e measurements ; most D_e estimates were based on a preheat of 260°C, while 3% of the estimates were from aliquots used for the preheat-plateau tests with lower preheat temperatures. Further dose-recovery measurements were undertaken for at least three aliquots per sample for samples measured at NCLR, with a preheat and cut-heat temperature of 260 and 220°C, respectively. These data are summarized as a histogram in Figure 5d with a mean of 1.01 ± 0.02 (n=58), showing that our chosen measurement protocol is able to accurately recover a known dose given before any thermal treatment.

7. Quartz optical ages and reliability

Quartz luminescence ages (Table 2) are based on the dose rates from Table 1 and the D_e estimates in Table 2. The two ages from UFV, JD-01 on basal sand and JD-03 on post-lake

deposits, are indistinguishable from the ages for stratigraphically equivalent samples run at NCLR. Ages range from 46.6 ± 4.5 ka to 18.7 ± 1.7 ka for samples from below and within the glaciolacustrine deposits, and 11.9 ± 1.2 ka to 10.6 ± 0.9 ka for sediments overlying the glaciolacustrine deposits. However, the reliability of these ages must be discussed before considering the geological implications.

7.1 Were the quartz grains well bleached before deposition?

In water-borne sediments the most frequently considered source of potential inaccuracy is incomplete resetting of the quartz OSL signal before deposition and burial. One method for testing the assumption of quartz signal resetting relies on the observation that the IRSL signals from feldspar are significantly more difficult to reset by daylight than the OSL from quartz (e.g. Godfrey-Smith et al., 1988; Murray et al., 2012). Thus, in principle, if quartz and feldspar ages agree, one can infer that the quartz grains must have been fully reset at deposition (Murray et al., 2012). Feldspar IRSL signals, however, are usually unstable (e.g., Huntley and Lamothe, 2001) and apparent ages derived from well-bleached feldspar will systematically underestimate ages based on well bleached quartz, unless the former are corrected for this fading (Huntley and Lamothe, 2001). But by considering the differential bleaching and fading rates between quartz and feldspar, Murray et al. (2012) concluded that if a feldspar IRSL age is consistent with or less than the corresponding quartz age, the quartz is very likely to have been sufficiently reset prior to deposition, an approach now widely used to identify well-bleached quartz in various depositional environments (e.g. Buylaert et al., 2012; Colarossi et al., 2015; Reimann et al., 2015; Sohbati et al., 2016).

In this study, the D_e of K-feldspar fraction was measured using at least 3 aliquots of all samples. K-feldspar dose rates are derived by adding the internal beta dose rate arising from an

assumed 12.5 % K content (Huntley and Baril, 1997) to the quartz dose rates. The resulting feldspar apparent ages are summarized in Table 2 and plotted against the quartz ages in Figure 6. All the feldspar ages (n= 15) lie below the line of unit slope, with an average ratio of 0.53 (feldspar to quartz age). The only exception to this is the result from sample 167520 which lies above the unity line. We conclude from this that there is no evidence to suggest that our quartz ages are significantly affected by incomplete bleaching prior to burial.

8. Discussion

Optical dating of transgressive basal sand below glaciolacustrine silt and clay at Garden Gulch provides direct age control on initial establishment of glacial Lake Missoula at a deep-lake elevation of at least 1185 m, or >65 percent of the maximum lake capacity. The lake reached this level between 18.7 ± 1.7 to 23.1 ± 1.6 ka, or at a weighted average age of 21.1 ± 1.5 ka (n = 4) (Table 2, Fig. 7). Seven optical ages for periglacially modified glaciolacustrine deposits range from 18.1 ± 1.3 to 23.6 ± 1.8 ka. At one standard error, the seven ages are equivalent, and equal to the basal sand ages (Figs. 7, 8). A weighted average age for the 11 samples is 20.9 ± 1.3 ka, as shown on Figures 7 and 8.

Each of the 12 cycles of glaciolacustrine deposits, "*a*" to "*l*", formed during transgressing, deepening, and retreating glacial Lake Missoula cycles, and resulted in exposed lake floors. Complex disruption of the sediments in the upper portions of cycles "*d*", "*e*", and "*j*" (section II, Fig. 3) may represent sediment accumulating during lake-level fluctuation and cryoturbation, forming syngenetic sand wedges. The time represented by the glaciolacustrine section is difficult to assess between the basal sand and the uppermost dated glaciolacustrine sequence at the top of cycle "*f*" (samples 167504 and 167505), as interpretation of varves is problematic and much of the sediment is deformed (Smith, 2017). The 11 fining-upward

sedimentary sequences capped by cryoturbation must represent at least one year of freezing and thawing to create the wedge structures, but they could have taken a few to a few tens of years to form. Because little sand was observed in exposures of the upper cycles "*g, h, i, j, and k*", they were not sampled, and the ages for the latest fluctuations in lake levels at the site are unknown. Of the nine ages from the glaciolacustrine section, two (167516 and 167520) are unreasonably old, likely due to remobilization and fluidization of a sand body as a subaqueous deposit.

The optical ages of 10.6 ± 0.9 ka (JD-03) to 12.6 ± 0.8 ka (167522) are consistent with the ages of post-glacial deposits. Although the lowest sample (167522) is from glaciolacustrine sediments of cycle "*l*", sand in the deposit was brought down from overlying slopewash in burrows, so the age is of the slopewash. A significant regional marker for the minimum age of glacial Lake Missoula sedimentation is the Glacier Peak "G" tephra. The tephra is within fluvial deposits on terraces ~2 m above the Flathead River, and inset ~100 m below the top of glaciolacustrine deposits in the Flathead River valley (Fig. 1; Levish, 1997; Hendrix, 2011; Hofmann and Hendrix, 2010). Thus, the final draining of the lake was prior to eruption of Glacier Peak "G" tephra at 13.7-13.4 cal. ka B.P. (Kuehn et al., 2009; Fig. 8).

In previous studies, glacial Lake Missoula was constrained by few numerical ages (Fig. 8). Previously published ages from glaciolacustrine sediments include one ^{14}C age (Hofmann and Hendrix, 2010) and three optical ages on quartz (Hanson et al., 2012). Hofmann and Hendrix (2010) report a 14,150 ± 50 cal. yr B.P. age for a pine needle collected from near the top of a core in the southern part of Flathead Lake, but below the Glacier Peak "G" tephra (Figs. 1, 8). This age shows that the glaciolacustrine deposits below the Glacier Peak "G" tephra represent deposition after retreat of the Flathead Lobe of the Cordilleran ice sheet (Hofmann and Hendrix, 2010). The lake was either glacial Lake Missoula, dammed by the Purcell Lobe, or in the locally

dammed proglacial Lake Flathead (Konizeski et al., 1968; Smith, 2004; Hofmann and Hendrix, 2010).

Hanson et al. (2012) reported an optical age on quartz from alluvium below glacial Lake Missoula deposits at the Ninemile section (15.1 ± 0.6 ka) and two on sand beds within the Rail Line section (Figs. 1, 8; 12.6 ± 0.6 ka and 14.8 ± 0.7 ka). The lower age from the Rail Line section is out of stratigraphic order and younger than the Glacier Peak "G" tephra. Discounting the younger age, this suggests that these lower elevation glaciolacustrine deposits may represent a late-lake history. Earlier glaciolacustrine deposits correlative with the Garden Gulch section may have been eroded by drainage of large, deeper lakes represented by the higher elevation deposits at Garden Gulch. Such erosion of low-elevation sediments in downstream reaches is consistent with modeling of glacial Lake Missoula outflows resulting from sudden releases during lake highstands (Alho et al., 2010). High magnitude draining of glacial Lake Missoula formed giant gravel bedforms that underlie the glaciolacustrine sediments in the canyon reaches of the lower Clark Fork River (Smith, 2006). Without additional geochronological data and correlations with other sections, it is unclear how many complete lake-filling and -draining cycles or only partial draining cycles are recorded in any of the glaciolacustrine silt and clay sections.

Optical ages for initial transgression of the glacial lake at the Garden Gulch location are consistent with the sparse chronology of advance of the Purcell Lobe of the Cordilleran Ice sheet. The age of advance of the Purcell Lobe into the ice dam region is constrained by a ^{14}C age of <22.8 cal. ka B.P for pre-glacial deposits that were later overridden during the advance (Fig. 8) (Clague et al., 1980). Retreat of the glacier from its maximum extent was dated at 15.7 ± 1.3 ka

(Breckenridge and Phillips, 2010) after recalculation of the five ^{10}Be ages on boulders on a lateral moraine (Balbas et al., 2017) (Fig. 8).

Sedimentological correlation, essentially event correlation, with dated strata in the Channeled Scabland of Washington and Oregon states has been the main method of inferring ages for lake-level changes in the Lake Missoula basin. The ages at Garden Gulch are consistent with the earliest ages of ~19 cal. ka B.P for last-glacial flooding in the Channeled Scabland (Fig. 8; Benito and O'Connor, 2003; O'Connor and Benito, 2009; Waitt, 2016) and with the 18.2 ± 1.5 ka age for one of the largest floods documented in the Channeled Scabland (Balbas et al., 2017).

From sedimentation events recognized in glacial Lake Columbia, Atwater (1986, 1987) argued that glacial Lake Missoula discharged 89 times into central Washington beginning about 17 cal. ka B.P. (from maximum ages on detrital wood; Fig. 8) and decreased in magnitude over time. Balbas et al. (2017) concluded that glacial Lake Missoula floods continued until 14.7 ± 1.2 ka. Benito and O'Connor (2003) summarized that most, if not all, of the last-glacial flood deposits along the Columbia River valley were emplaced after 22,870 ± 316 cal. yr B.P., that floods continued through 14,612 ± 165 cal. yr B.P., and that flood magnitude generally decreased over time.

Low-salinity anomalies in the north Pacific, dated at 24–17 cal. ka B.P. (Lopes and Mix, 2009) and correlations of offshore sands in core at ~19.3–~14.9 cal. ka B.P. (Gombiner et al., 2016), and with a major deposit in the Escanaba Trough (Zuffa et al., 2000) have been ascribed to floods from glacial Lake Missoula (Hendy, 2009; Lopes and Mix, 2009; Baker et al., 2016; Gombiner et al., 2016). The optical ages for initial transgression at Garden Gulch, the maximum age for late-glacial catastrophic flooding in the Columbia River Gorge of <22 cal. ka B.P. of Benito and O'Connor (2003), and the date for the large 18.2 ± 1.5 ka flood are consistent with

the ages of the lower six fluctuations in lake level expressed in the Garden Gulch section. The Garden Gulch section represents the earliest filling and draining cycles in the last-glacial episode of flooding in the Channeled Scabland (Fig. 8).

9. Conclusions

Glaciolacustrine sediments preserved at high elevations within the ~9,500 km^2 glacial Lake Missoula impoundment record initial late Pleistocene transgression, deepening, lake lowering, and lake draining. Twelve sedimentary cycles were deposited at the Garden Gulch section during periods of lake deepening and lake-level lowering. Each of the lake-level lowerings below an altitude of about 1185 m permitted periglacial features to develop, which trapped sand grains of quartz and feldspar in the lower six cycles.

Seventeen samples for optical dating were collected at eight stratigraphic levels in order to provide a chronology for the lower six, of the twelve, lake-level cycles at Garden Gulch. Four ages on the basal sand and seven ages from the glaciolacustrine section suggest that these units are essentially contemporaneous with an age of 20.9 ± 1.3 ka (n=11). The sedimentological considerations together with chronology suggest that the time represented by the lower six cycles in the section may range between decades to ~2 ka. Additional chronology of the upper six cycles is needed.

The uppermost glaciolacustrine cycle is burrowed and pedogenically modified and capped by the post-lake sediment. Three ages from the slopewash and underlying disturbed glaciolacustrine sediment range from 10.6 ± 0.9 to 12.6 ± 0.8 ka. These ages are consistent with the cessation of glaciolacustrine deposition before eruption of the Glacier Peak “G” tephra (13.7-13.4 cal. ka B.P.).

The stratigraphy and dating of the Garden Gulch section provides a record of glacial Lake Missoula repeatedly attaining high elevation and deep lake levels in the late Pleistocene. Sediments were deposited in <100 m of water at an elevation that would have contained >65 percent of the maximum water volume of glacial Lake Missoula. The timing and stratigraphy are consistent with the available chronology of the damming by the Cordilleran ice sheet and downstream megaflood deposits formed by repeated cataclysmic ice-dam breaching and drainage of glacial Lake Missoula. One or more catastrophic drainings from lake-level stands that deposited the sediments at Garden Gulch could be responsible for eroding glaciolacustrine deposits downstream, thus the glaciolacustrine sediments in the lake basin are likely time-transgressive. Still uncertain are the number of full versus partial lake drainages represented in any of the glaciolacustrine sections.

Acknowledgements

Discussions of various field sites in the glacial Lake Missoula basin with Vic Baker, Don Winston, Michelle Hanson, Sid Hemming, Scott Stine, Joel Gombiner, and others were important to work on problems presented here. Reviews of the manuscript by Jim O'Connor and Martin Margold substantially improved the clarity of the manuscript. Optical dating was partially funded by a New Faculty Seed and Faculty Development grants from Montana Tech of The University of Montana to LNS. Optical dating at the NCLR was assisted by Louise Helsted, Vicki Hansen, and Eun-Young Yeo. Optical dating at the Luminescence Dating Laboratory at University of the Fraser Valley is supported in part by a Natural Science and Engineering Research Council (NSERC) of Canada Discovery Grant and a NSERC Research Tools and Instruments Grant to OBL. Justine Riches (née Cullen) and Christina Neudorf were instrumental

in sample preparation and measurements. Without the generous cooperation of the landowner, Mr. Jim Davis, this study would not have been possible.

References

Alho, P., Baker, V.R., Smith, L.N., 2010. Paleohydraulic reconstruction of the largest Glacial Lake Missoula draining(s). Quat. Sci. Rev. 29, 3067–3078. doi:10.1016/j.quascirev.2010.07.015

Atwater, B.F., 1987. Status of glacial Lake Columbia during the last floods from glacial Lake Missoula. Quat. Res. 27, 182–201.

Atwater, B.F., 1986. Pleistocene Glacial-Lake Deposits of the Sanpoil River Valley , Northeastern Washington. U.S. Geol. Surv. 1661.

Atwater, B.F., 1984. Periodic floods from glacial Lake Missoula into the Sanpoil arm of glacial Lake Columbia, northeastern Washington. Geology 12, 464–467. doi:10.1130/0091-7613(1984)12<464:PFFGLM>2.0.CO;2

Baker, V.R., 1973. Paleohydrology and Sedimentology of Lake Missoula Flooding in Eastern Washington, Geological Society of America Special Papers. Geological Society of America. doi:10.1130/SPE144-p1

Baker, V.R., Bjornstad, B.N., Gaylord, D.R., Smith, G.A., Meyer, S.E., Alho, P., Breckenridge, R.M., Sweeney, M.R., Zreda, M., 2016. Pleistocene megaflood landscapes of the Channeled Scabland, in: Exploring the Geology of the Inland Northwest. Geological Society of America, pp. 1–73. doi:10.1130/2016.0041(01)

Baker, V.R., Bunker, R.C., 1985. Cataclysmic late Pleistocene flooding from glacial Lake Missoula: A review. Quat. Sci. Rev. 4, 1–41. doi:10.1016/0277-3791(85)90027-7

Balbas, A.M., Barth, A.M., Clark, P.U., Clark, J., Caffee, M., O'Connor, J., Baker, V.R., Konrad, K., Bjornstad, B., O'Connor, J., Baker, V.R., Konrad, K., Bjornstad, B., 2017. 10Be dating of late Pleistocene megafloods and Cordilleran Ice Sheet retreat in the northwestern United States. Geology 45.

Benito, G., O'Connor, J.E., 2003. Number and size of last-glacial Missoula floods in the Columbia River valley between the Pasco Basin, Washington, and Portland, Oregon. Bull. Geol. Soc. Am. 115, 624–638. doi:10.1130/0016-7606(2003)115<0624:NASOLM>2.0.CO;2

Berg, R.B., 2006. Geologic map of the Upper Clark Fork Valley between Bearmouth and Missoula, southwestern Montana. Montana Bureau of Mines and Geology, Butte.

Berg, R.B., 2005. Geologic map of the Upper Clark Fork Valley between Garrison and Bearmouth, southwestern Montana, Open-File Report. Montana Bureau of Mines and Geology, Butte.

Breckenridge, R.M., Atwater, B.F., Baker, V.R., Busacca, A.J., Chambers, R.L., Curry, R.R., Hanson, L.G., Kever, E.P., McDonald, E. V., Stradling, D.F., Waitt, R.B., 1989. Glacial Lake Missoula and the Channeled Scabland, in: International Geological Congress, 28th, Guidebook. American Geophysical Union, Washington D.C., p. 72. doi:10.1029/FT310

Breckenridge, R.M., Phillips, W.M., 2010. New cosmogenic (super 10) Be surface exposure ages for the Purcell Trench Lobe of the Cordilleran ice sheet in Idaho - GeoRef - ProQuest, in: Abstracts with Programs. Geological Society of America, p. 309.

Bretz, J.H., 1969. The Lake Missoula floods and the channeled scabland. J. Geol. 77, 505–543.

Buylaert, J.P., Jain, M., Murray, A.S., Thomsen, K.J., Thiel, C., Sohbati, R., 2012. A robust feldspar luminescence dating method for Middle and Late Pleistocene sediments. Boreas

41, 435–451. doi:10.1111/j.1502-3885.2012.00248.x

Campbell, M.R., others, and, 1915. Guidebook of the Western United States: Part A - The Northern Pacific Route, With a Side Trip to Yellowstone Park. Bulletin 611, 212.

Carrara, P.E., Kiver, E.P., Stradling, D.F., 1996. The southern limit of Cordilleran ice in the Colville and Pend Oreille valleys of northeastern Washington during the Late Wisconsin glaciation. Can. J. Earth Sci. 33, 769–778. doi:10.1139/e96-059

Clague, J.J., Armstrong, J.E., Mathews, W.H., 1980. Advance of the late Wisconsin Cordilleran Ice Sheet in southern British Columbia since 22,000 Yr B.P. Quat. Res. 13, 322–326. doi:10.1016/0033-5894(80)90060-5

Clague, J.J., Barendregt, R., Enkin, R.J., Foit, F.F., 2003. Paleomagnetic and tephra evidence for tens of Missoula floods in southern Washington. Geology 31, 247. doi:10.1130/0091-7613(2003)031<0247:PATEFT>2.0.CO;2

Colarossi, D., Duller, G.A.T., Roberts, H.M., Tooth, S., Lyons, R., 2015. Comparison of paired quartz OSL and feldspar post-IR IRSL dose distributions in poorly bleached fluvial sediments from South Africa. Quat. Geochronol. 30, 233–238. doi:10.1016/j.quageo.2015.02.015

Cunningham, A.C., Wallinga, J., 2010. Selection of integration time intervals for quartz OSL decay curves. Quat. Geochronol. 5, 657–666. doi:10.1016/j.quageo.2010.08.004

Duller, G.A.T., 2003. Distinguishing quartz and feldspar in single grain luminescence measurements. Radiat. Meas. 37, 161–165. doi:10.1016/S1350-4487(02)00170-1

Godfrey-Smith, D.I., Huntley, D.J., Chen, W.H., 1988. Optical dating studies of quartz and feldspar sediment extracts. Quat. Sci. Rev. 7, 373–380. doi:10.1016/0277-3791(88)90032-7

Gombiner, J.H., Hemming, S.R., Hendy, I.L., Bryce, J.G., Blichert-Toft, J., 2016. Isotopic and

elemental evidence for Scabland Flood sediments offshore Vancouver Island. Quat. Sci. Rev. 139, 129–137. doi:10.1016/j.quascirev.2016.02.026

Guérin, G., Mercier, N., Adamiec, G., 2011. Dose-rate conversion factors: update. Anc. TL 29, 5–8.

Hansen, V., Murray, A., Buylaert, J.P., Yeo, E.Y., Thomsen, K., 2015. A new irradiated quartz for beta source calibration. Radiat. Meas. 81, 123–127. doi:10.1016/j.radmeas.2015.02.017

Hanson, M.A., Clague, J.J., 2016. Record of glacial Lake Missoula floods in glacial Lake Columbia, Washington. Quat. Sci. Rev. 133, 62–76. doi:10.1016/j.quascirev.2015.12.009

Hanson, M.A., Lian, O.B., Clague, J.J., 2012. The sequence and timing of large late Pleistocene floods from glacial Lake Missoula. Quat. Sci. Rev. 31, 67–81. doi:10.1016/j.quascirev.2011.11.009

Hendrix, M.S., 2011. Geologic map of Niarada, Irvine Hills, and Hot Springs NE USGS 7.5' quadrangles and parts of Elmo, Irvine Lookout Tower, Bu alo Bridge, Rollins, Proctor, Lake Mary Ronan and Ko ord Ridge USGS 7.5' quadrangles 20230.

Hendy, I., 2009. A fresh perspective on the Cordilleran Ice Sheet. Geology 37, 95–96. doi:10.1130/focus012009.1

Hofmann, M.H., Hendrix, M.S., 2010. Depositional processes and the inferred history of ice-margin retreat associated with the deglaciation of the Cordilleran Ice Sheet: The sedimentary record from Flathead Lake, northwest Montana, USA. Sediment. Geol. 223, 61–74. doi:10.1016/j.sedgeo.2009.10.004

Huntley, D., Baril, M., 1997. The K content of the K-feldspars being measured in optical dating or in thermoluminescence dating. Anc. TL 15, 11–13.

Huntley, D.J., Lamothe, M., 2001. Ubiquity of anomalous fading in K-feldspars and the

measurement and correction for it in optical dating. Can. J. Earth Sci. 38, 1093–1106. doi:10.1139/cjes-38-7-1093

Jain, M., Murray, A.S., Bøtter-Jensen, L., 2003. Characterisation of blue-light stimulated luminescence components in different quartz samples: Implications for dose measurement. Radiat. Meas. 37, 441–449. doi:10.1016/S1350-4487(03)00052-0

Konizeski, R.L., Brietkrietz, A., McMurtrey, R.G., 1968. Geology and ground water resources of the Kalispell Valley, northwestern Montana. Montana Bureau of Mines and Geology Bulletin 68, Butte.

Kuehn, S.C., Froese, D.G., Carrara, P.E., Foit, F.F., Pearce, N.J.G., Rotheisler, P., 2009. Major- and trace-element characterization, expanded distribution, and a new chronology for the latest Pleistocene Glacier Peak tephras in western North America. Quat. Res. 71, 201–216. doi:10.1016/j.yqres.2008.11.003

Levish, D.R., 1997. Late Pleistocene sedimentation in glacial Lake Missoula and revised glacial history of the Flathead Lobe of the Cordilleran Ice Sheet, Mission valley, Montana. Boulder.

Lonn, J.D., McDonald, C., Sears, J.W., Smith, L.N., 2010. Geologic map of the Missoula East 30’ x 60’ quadrangle, western Montana, Open-File Report. Butte.

Lonn, J.D., Smith, L.N., McCulloch, R.B., 2007. Geologic map of the Plains 30’ x 60’ quadrangle, western Montana, Open-File Report. Butte.

Lopes, C., Mix, A.C., 2009. Pleistocene megafloods in the Northeast Pacific. Geology 37, 79–82. doi:10.1130/G25025A.1

Murray, A.S., Marten, R., Johnston, A., Martin, P., 1987. Analysis for naturally occuring radionuclides at environmental concentrations by gamma spectrometry. J. Radioanal. Nucl.

Chem. Artic. 115, 263–288. doi:10.1007/BF02037443

Murray, A.S., Thomsen, K.J., Masuda, N., Buylaert, J.P., Jain, M., 2012. Identifying well-bleached quartz using the different bleaching rates of quartz and feldspar luminescence signals. Radiat. Meas. 47, 688–695. doi:10.1016/j.radmeas.2012.05.006

O'Connor, Jim E; Benito, G.A., 2009. Late Pleistocene Missoula floods; 15,000-20,000 calendar years before present from radiocarbon dating. Abstr. with Programs - Geol. Soc. Am. 41, 169.

O'Connor, J.E., Baker, V.R., 1992. Magnitudes and implications of peak discharges from glacial Lake Missoula. Geol. Soc. Am. Bull. 104, 267–279. doi:10.1130/0016-7606(1992)104<0267:MAIOPD>2.3.CO;2

Pardee, J.T., 1942. Unusual Currents in Glacial Lake Missoula, Montana. Bull. Geol. Soc. Am. 53, 1569–1600.

Pardee, J.T., 1910. The Glacial Lake Missoula. J. Geol. 18, 376–386.

Prescott, J.R., Hutton, J.T., 1994. Cosmic ray contributions to dose rates for luminescence and ESR dating: Large depths and long-term time variations. Radiat. Meas. 23, 497–500. doi:10.1016/1350-4487(94)90086-8

Reimann, T., Notenboom, P.D., De Schipper, M.A., Wallinga, J., 2015. Testing for sufficient signal resetting during sediment transport using a polymineral multiple-signal luminescence approach. Quat. Geochronol. 25, 26–36. doi:10.1016/j.quageo.2014.09.002

Reimer, P.J., Bard, E., Bayliss, A., Beck, J.W., Blackwell, P.G., Ramsey, C.B., Buck, C.E., Cheng, H., Edwards, R.L., Friedrich, M., Grootes, P.M., Guilderson, T.P., Haflidason, H., Hajdas, I., Hatté, C., Heaton, T.J., Hoffmann, D.L., Hogg, A.G., Hughen, K.A., Kaiser, K.F., Kromer, B., Manning, S.W., Niu, M., Reimer, R.W., Richards, D.A., Scott, E.M.,

Southon, J.R., Staff, R.A., Turney, C.S.M., van der Plicht, J., 2013. IntCal13 and Marine13 Radiocarbon Age Calibration Curves 0–50,000 Years cal BP. Radiocarbon 55, 1869–1887. doi:10.2458/azu_js_rc.55.16947

Roberts, R.G., Lian, O.B., 2015. Dating techniques: Illuminating the past. Nature 520, 438–439. doi:10.1038/520438a

Singarayer, J.S., Bailey, R.M., 2003. Further investigations of the quartz optically stimulated luminescence components using linear modulation. Radiat. Meas. 37, 451–458. doi:10.1016/S1350-4487(03)00062-3

Smith, L.N., 2017. Repeated sedimentation and exposure of glacial Lake Missoula sediments: A lake-level history at Garden Gulch, Montana, USA. Quat. Sci. Rev. 155, 114–126. doi:10.1016/j.quascirev.2016.11.018

Smith, L.N., 2006. Stratigraphic evidence for multiple drainings of glacial Lake Missoula along the Clark Fork River, Montana, USA. Quat. Res. 66, 311–322. doi:10.1016/j.yqres.2006.05.009

Smith, L.N., 2004. Late Pleistocene stratigraphy and implications for deglaciation and subglacial processes of the Flathead Lobe of the Cordilleran Ice Sheet, Flathead Valley, Montana, USA. Sediment. Geol. 165. doi:10.1016/j.sedgeo.2003.11.013

Smith, L.N., Hanson, M.A., 2014. Sedimentary record of glacial Lake Missoula along the Clark Fork River from deep to shallow positions in the former lakes: St. Regis to near Drummond, Montana, in: Shaw, C.A., Tikoff, B. (Eds.), Exploring the Northern Rocky Mountains. Geological Society of America, pp. 51–63. doi:10.1130/9780813700373

Sohbati, R., Borella, J., Murray, A., Quigley, M., Buylaert, J.P., 2016. Optical dating of loessic hillslope sediments constrains timing of prehistoric rockfalls, Christchurch, New Zealand. J.

Quat. Sci. 31, 678–690. doi:10.1002/jqs.2895

Thomsen, K.J., Murray, A.S., Buylaert, J.P., Jain, M., Hansen, J.H., Aubry, T., 2016. Testing single-grain quartz OSL methods using sediment samples with independent age control from the Bordes-Fitte rockshelter (Roches d'Abilly site, Central France). Quat. Geochronol. 31, 77–96. doi:10.1016/j.quageo.2015.11.002

Waitt, R.B., 2016. Megafloods and Clovis cache at Wenatchee, Washington. Quat. Res. 85, 430–444. doi:10.1016/j.yqres.2016.02.007

Waitt, R.B., 1985. Case for periodic, colossal jökulhlaups from Pleistocene glacial Lake Missoula. Geol. Soc. Am. Bull. 96, 1271–1286. doi:10.1130/0016-7606(1985)96<1271:CFPCJF>2.0.CO;2

Waitt, R.B., 1980. About forty last-glacial Lake Missoula jökulhlaups through southern Washington. J. Geol. 88, 653–679.

Waitt, R.B., Denlinger, R.P., O'Connor, J.E., 2009. Volcanoes to Vineyards: Geologic Field Trips through the Dynamic Landscape of the Pacific Northwest, Field Guides. Geological Society of America. doi:10.1130/2009.fld015(33)

Wallinga, J., Murray, A., Wintle, A., 2000. The single-aliquot regenerative-dose (SAR) protocol applied to coarse-grain feldspar. Radiat. Meas. 32, 529–533. doi:10.1016/S1350-4487(00)00091-3

Wintle, A.G., Murray, A.S., 2006. A review of quartz optically stimulated luminescence characteristics and their relevance in single-aliquot regeneration dating protocols. Radiat. Meas. 41, 369–391. doi:10.1016/j.radmeas.2005.11.001

Wintle, A.G., Murray, A.S., 2000. Quartz OSL: Effects of thermal treatment and their relevance to laboratory dating procedures. Radiat. Meas. 32, 387–400. doi:10.1016/S1350-

4487(00)00057-3

Zuffa, G.G., Normark, W.R., Serra, F., Brunner, C.A., 2000. Turbidite Megabeds in an Oceanic Rift Valley Recording Jokulhlaups of Late Pleistocene Glacial Lakes of the Western United States. J. Geol. 108, 253–274.

FIGURE CAPTIONS

Figure 1. (A) Location map of glacial Lake Missoula, key stratigraphic sections, maximum extent of late Pleistocene glacial ice, approximate outline of Purcell Trench lobe ice dam, and the present study area along the Clark Fork River; Flathead Lake core location of Hofmann and Hendrix (2010) shown; dashed line shows possible retreat position of ice when glacial Lake Missoula extended farther north. (B) Relationship between of volume and altitude of the lake calculated at six discrete lake elevations from present topography (modified from Smith, 2006); m asl – meters above sea level.

Figure 2. Geologic map of study area; numbers I, II, and III show locations of measured sections where samples for optical dating were collected; topographic contour interval of 50 m; geologic contacts modified from Berg (2005).

Figure 3. Graphical logs of measured sections and stratigraphic positions of samples for optical dating shown by black arrows (locations in Fig. 2). (I) Section I of the lower unconsolidated units at Garden Gulch measured at the location of optical dating sample JD-01; modified from Smith (2017). (II) Section II is a composite section through the entire outcrop of glaciolacustrine deposits; white arrows indicate exposure-surface horizons, dashed arrows point to aggradational surfaces at the top of cycles *“d”, “e”, and “j”*; modified from Smith (2017). (III) Section III measured in glaciolacustrine sediments above weathered bedrock in the westernmost railroad cut outcrop.

Figure 4. Examples of sedimentary facies in measured sections and locations of samples; vertical measurements correspond to height above base of measured sections in Figure 3. (A) Laminated and cross laminated sand and silt at 0.5-1.0 m in section II; sample JD-2 was from the climbing rippled unit at 65 cm. (B) Overview of alluvium of the paleo-Clark Fork River, deposits of the initial glacial Lake Missoula transgression, and overlying glaciolacustrine deposits at section I, looking north; black arrow points to bedded silt interlayered with sandy gravel; the JD-1 sample for optical dating was collected in the sandy unit at the point of the trowel (handle is 13 cm long). (C) Laminated glaciolacustrine silt and clay overlie transgressing lake alluvium above paleo-Clark Fork River alluvium; black arrow as above, white arrow points to intraclast of laminated silt within alluvium. (D) Overview of the lower part of section II (Fig. 3) showing locations of three photographs and samples for optical dating. (E) Sampling tube for 167501 before excavation of gravelly silt and sand in downward-tapering wedge at the top of cycle *"b"* section 2 (Fig. 3). (F) Location of sample 167503 at the top of cycle *"c"* (Fig. 3). (G) The uppermost samples collected for optical dating were taken from massive post-lake sediment above and below a paleosol horizon. (H) Overview of the upper part of section II showing the locations of seven samples and the location of Figure 4G.

Figure 5. (A) Representative dose-response and 'natural' OSL (inset) curves for sample 167501. The main graph shows data for an aliquot accepted for dating; the dose-response curve consists of sensitivity-corrected luminescence intensity (L_x/T_x) plotted as a function of laboratory beta dose. The equivalent dose (D_e) value for an individual aliquot is found by interpolating the luminescence intensity arising from the natural signal, shown by the horizontal line, onto the dose response curve. The inset compares the 'natural' OSL curve with that of Risø calibration quartz (Hansen et al., 2015), confirming a dominant fast component in our samples. (B) The

equivalent dose (D_e) and (C) dose-recovery preheat plateaus for sample 167502. Each data point is an average of at least three aliquots. The error bars represent one standard error. The dashed line in (B) represents the average D_e. The dashed lines in (C) show 10% of unity. (D) Histogram of dose recovery ratios of samples analyzed at NCLR.

Figure 6. Comparison of quartz OSL and K-feldspar IRSL ages; the inset shows all data (dashed line represents 1:1 relationship); see text for discussion.

Figure 7. Graphical summary of optical ages (error bars represent 1 standard error) and the stratigraphic context of section II (Figure 3); JD-01 and 167525 are projected onto the section relative to their position below glaciolacustrine deposits. The gray triangle near the top of the section represents possible ages of the upper glaciolacustrine cycles. The outlier age of 46.6 ± 4.5 ka for 167520 is not included in the plot and 167516 was contaminated by older sand (see text for explanation). The vertical gray line shows the weighted mean age of 20.9 ± 1.3 ka for the 11 ages. The age of the Glacier Peak "G" tephra from Kuehn et al. (2009) is shown by a vertical arrow.

Figure 8. Summary of a selection of relevant geochronologic data compared to approximate ages for advance and retreat of the Cordilleran Ice Sheet, shown by black and white bars (modified from Baker et al., 2016). (A) Times of glaciation (younger two ^{14}C ages suggesting active glaciers in southern British Columbia); the lower ^{14}C age indicates ice-free conditions in southeastern British Columbia (after Clague et al., 1980); the youngest age for corresponds to the age for beginning retreat of the Purcell lobe at the ice dam (Balbas et al., 2017). (B) ^{10}Be age on a late-glacial lateral moraine in the Purcell Trench at Lake Pend Oreille (Breckenridge and Phillips, 2010), recalculated by Balbas et al. (2017). (C) Age of a pine needle in the upper part of a glaciolacustrine section of Flathead Lake core (Fig. 1; Hofmann and Hendrix, 2010).

(D) Two ages from the glacial Lake Missoula deposits at the Ninemile and Rail Line sections (Hanson et al., 2012); see text for discussion. (E) Weighted average age (n=11) from this study on basal sand and glaciolacustrine sediments at Garden Gulch, and three ages of post-lake sediments. (F) Radiocarbon ages for organics below (lower one) or within megaflood deposits in the Colombia River gorge; vertical line suggest continuity of section (Benito and O'Connor, 2003). (G) Age of the Glacier Peak "G" tephra (Kuehn et al., 2009) is shown by the horizontal gray bar; it represents the minimum age for glacial Lake Missoula. (H) Radiocarbon ages and interpreted duration for the Manila Creek section of glacial Lake Columbia; vertical lines suggest continuity of section (Atwater, 1986). (I) Glacial Lake Missoula flood record in central Washington from ^{10}Be ages on boulders, a – age for early megaflood; b – age for last flood from glacial Lake Missoula (Balbas et al., 2017). (J) Glacial Lake Missoula flood record from offshore Vancouver Island, British Columbia (Gombiner et al., 2016). (K) Curve of practical salinity units (PSU) in the northeast Pacific, salinity decreases to the left (from Lopes and Mix, 2009).

TABLES

Table 1. Sample depths, radionuclide concentrations, water content, and total dose rates for gamma spectroscopy (GS) and Neutron Activation Analyses (NAA) analyses. Radionuclide concentrations were converted to dry infinite matrix dose rates using the conversion factors of Guérin et al. (2011).

Table 2. Dose rates, equivalent doses, and optical ages.

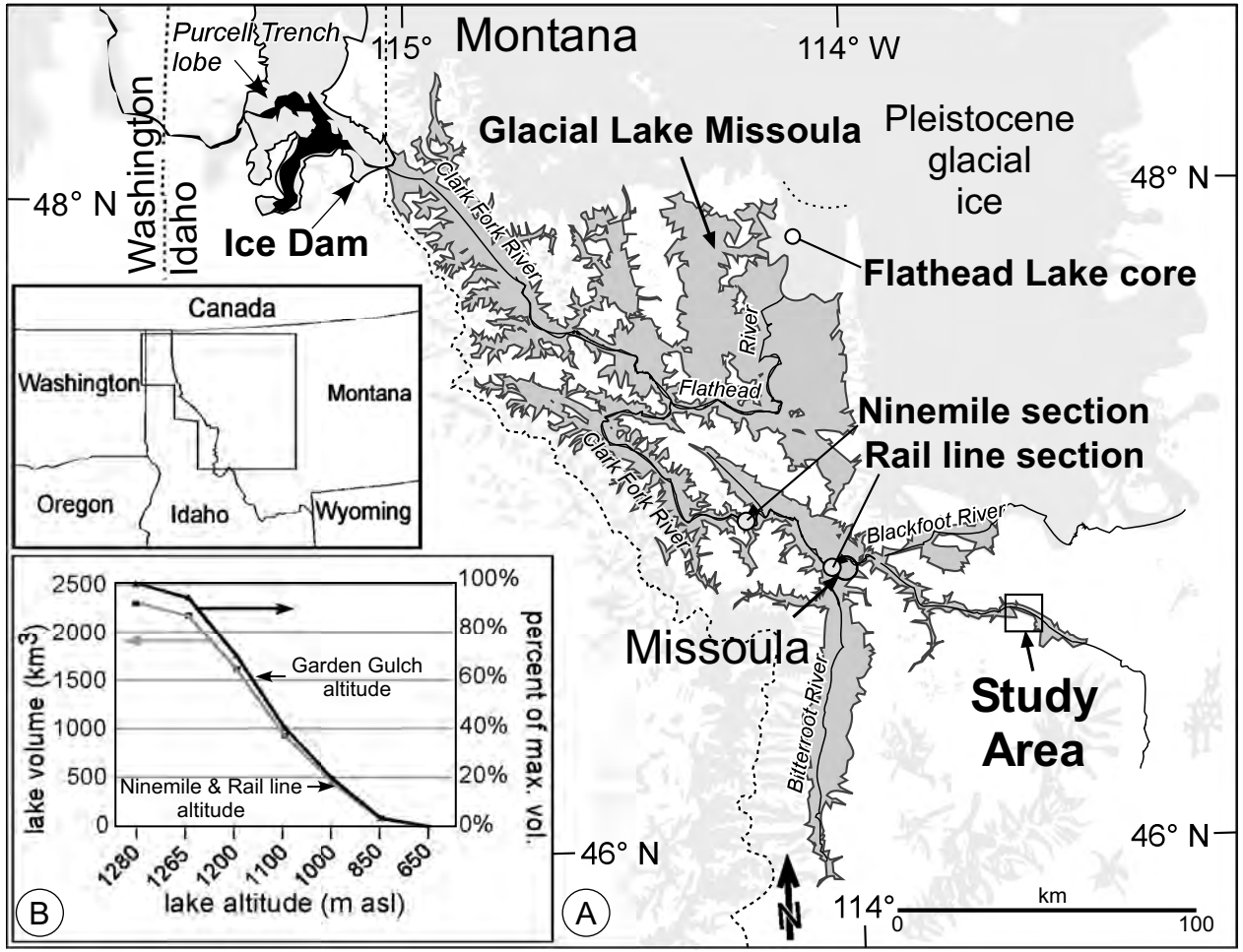
Montana
115°
114° W
Purcell Trench lobe
Washington
Idaho
Ice Dam
48° N
Glacial Lake Missoula
Pleistocene glacial ice
Clark Fork River
Flathead Lake core
Flathead River
Ninemile section
Rail line section
Blackfoot River
Missoula
Bitterroot River
Study Area
46° N
114°
km
0
100
Canada
Washington
Montana
Oregon
Idaho
Wyoming
lake volume (km3)
percent of max. vol.
Garden Gulch altitude
Ninemile & Rail line altitude
lake altitude (m asl)
2500
2000
1500
1000
500
0
100%
80%
60%
40%
20%
0%
1280
1265
1200
1100
1000
850
650
B
A

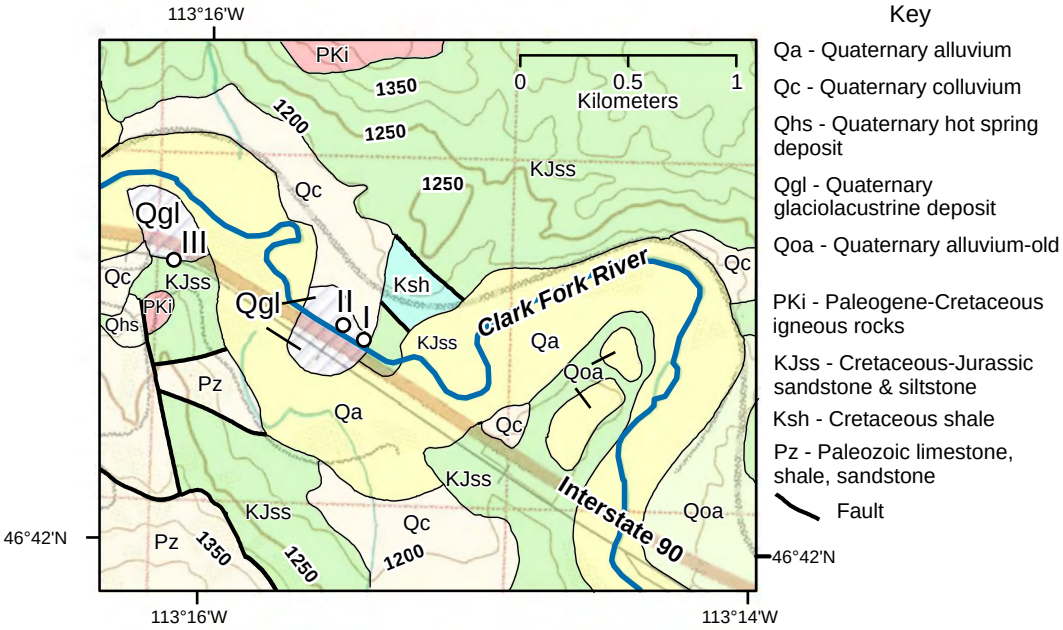
113°16'W
113°14'W
46°42'N
0
0.5
1
Kilometers
PKi
1350
1200
1250
KJss
Qc
Qgl
III
Qc
KJss
PKi
Qhs
Qgl
II
I
Ksh
KJss
Clark Fork River
Qa
Qc
Qoa
Pz
Qa
Qc
KJss
Interstate 90
Qoa
KJss
Qc
Pz
1350
1250
1200
Key
Qa - Quaternary alluvium
Qc - Quaternary colluvium
Qhs - Quaternary hot spring deposit
Qgl - Quaternary glaciolacustrine deposit
Qoa - Quaternary alluvium-old
PKi - Paleogene-Cretaceous igneous rocks
KJss - Cretaceous-Jurassic sandstone & siltstone
Ksh - Cretaceous shale
Pz - Paleozoic limestone, shale, sandstone
Fault

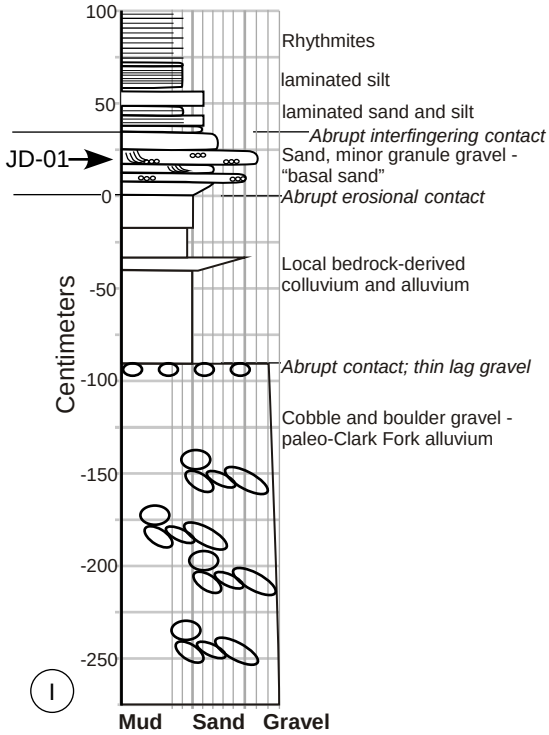
100
50
0
-50
-100
-150
-200
-250
Centimeters
JD-01
Rhythmites
laminated silt
laminated sand and silt
Abrupt interfingering contact
Sand, minor granule gravel - "basal sand"
Abrupt erosional contact
Local bedrock-derived colluvium and alluvium
Abrupt contact; thin lag gravel
Cobble and boulder gravel - paleo-Clark Fork alluvium
I
Mud
Sand
Gravel

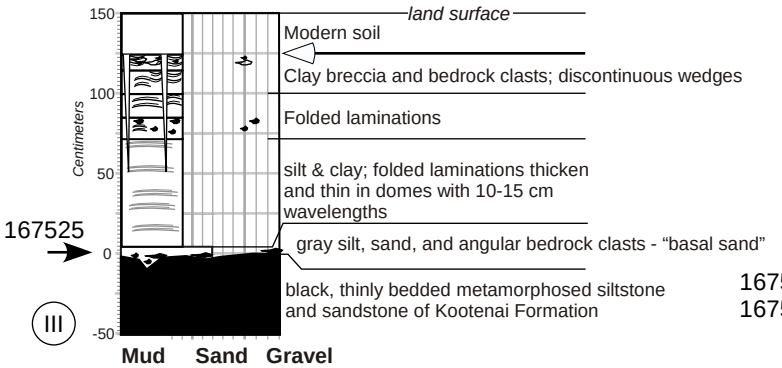
150
100
50
0
-50
Centimeters
167525
land surface
Modern soil
Clay breccia and bedrock clasts; discontinuous wedges
Folded laminations
silt & clay; folded laminations thicken and thin in domes with 10-15 cm wavelengths
gray silt, sand, and angular bedrock clasts - "basal sand"
black, thinly bedded metamorphosed siltstone and sandstone of Kootenai Formation
III
Mud
Sand
Gravel

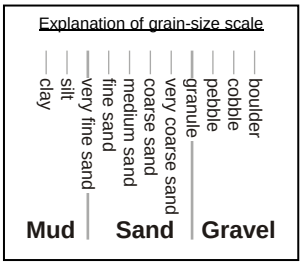
Explanation of grain-size scale
clay
silt
very fine sand
fine sand
medium sand
coarse sand
very coarse sand
granule
pebble
cobble
boulder
Mud
Sand
Gravel

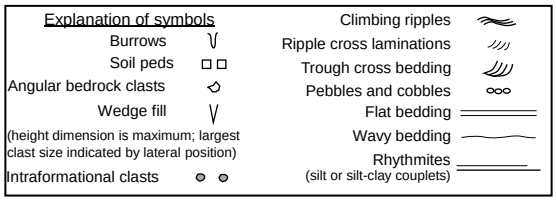
Explanation of symbols
Burrows
Soil peds
Angular bedrock clasts
Wedge fill
(height dimension is maximum; largest clast size indicated by lateral position)
Intraformational clasts
Climbing ripples
Ripple cross laminations
Trough cross bedding
Pebbles and cobbles
Flat bedding
Wavy bedding
Rhythmites
(silt or silt-clay couplets)

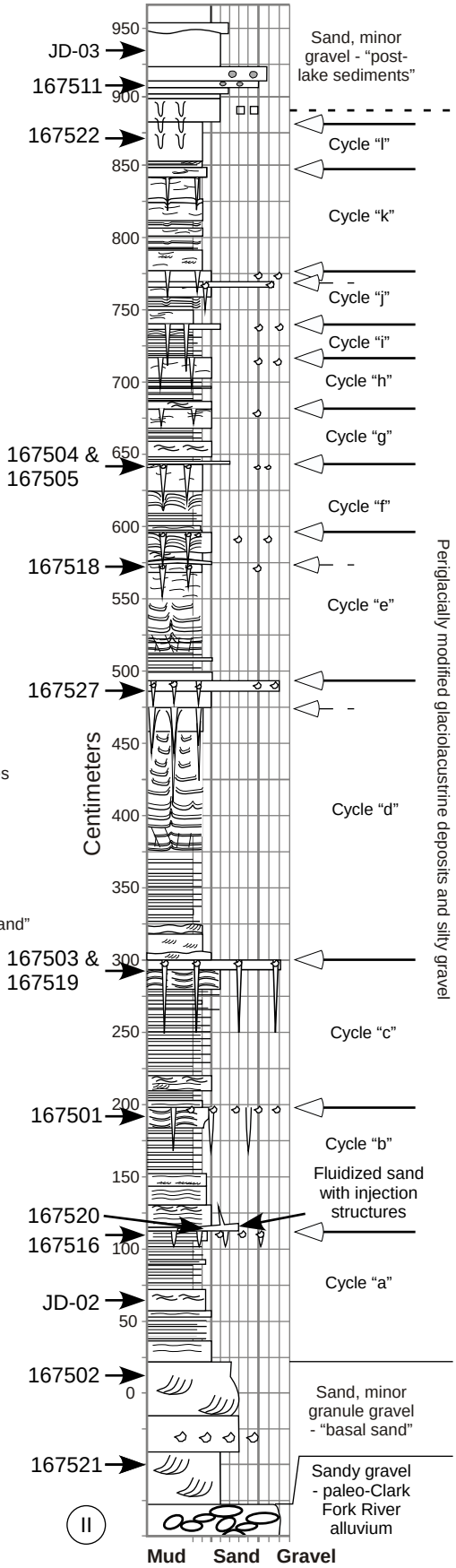
950
900
850
800
750
700
650
600
550
500
450
400
350
300
250
200
150
100
50
0
Centimeters
JD-03
167511
167522
167504 & 167505
167518
167527
167503 & 167519
167501
167520
167516
JD-02
167502
167521
Sand, minor gravel - "post-lake sediments"
Cycle "l"
Cycle "k"
Cycle "j"
Cycle "i"
Cycle "h"
Cycle "g"
Cycle "f"
Cycle "e"
Cycle "d"
Cycle "c"
Cycle "b"
Fluidized sand with injection structures
Cycle "a"
Sand, minor granule gravel - "basal sand"
Sandy gravel - paleo-Clark Fork River alluvium
Periglacially modified glaciolacustrine deposits and silty gravel
II
Mud
Sand
Gravel

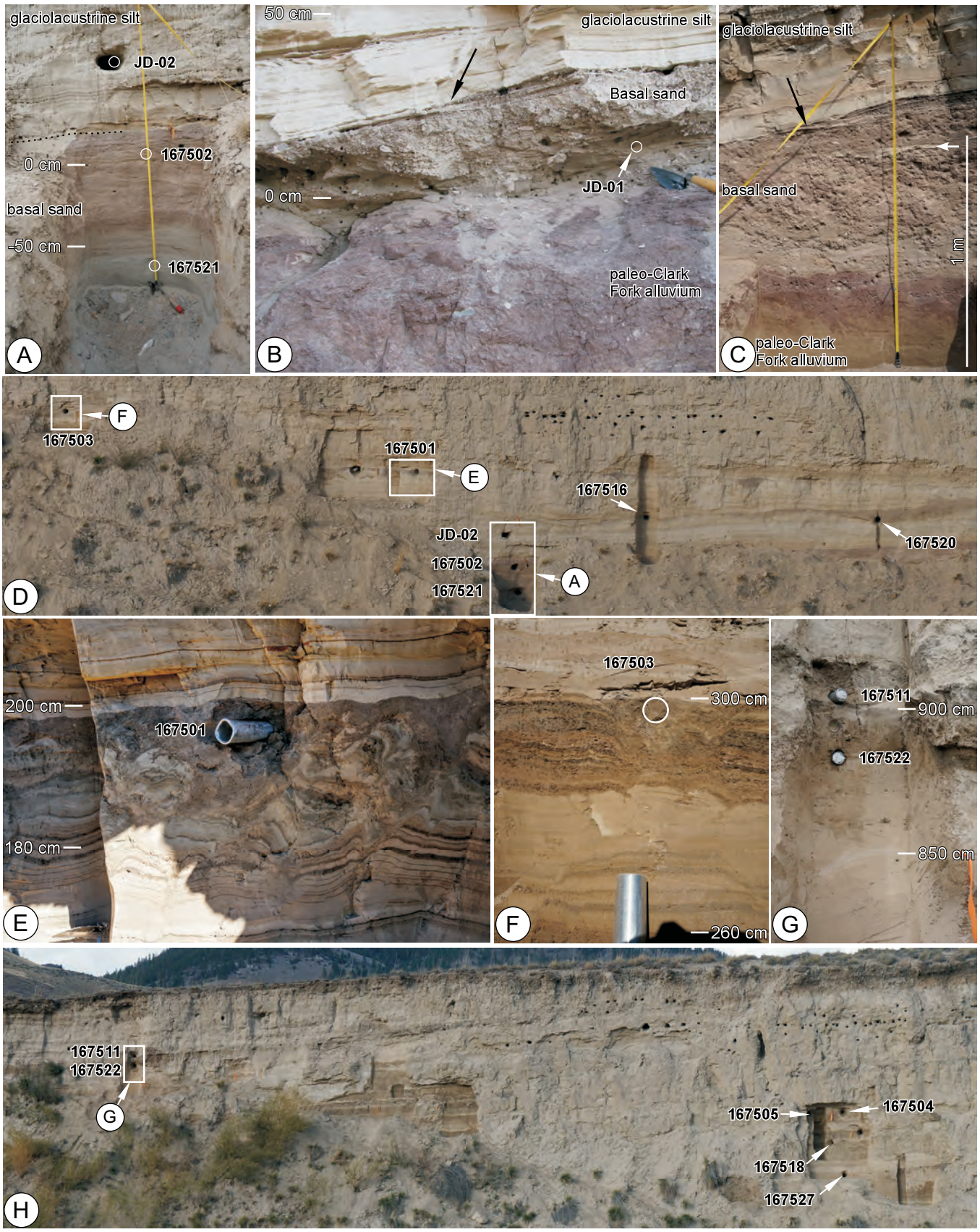
glaciolacustrine silt
JD-02
0 cm
167502
basal sand
-50 cm
167521
A
50 cm
glaciolacustrine silt
Basal sand
JD-01
0 cm
paleo-Clark
Fork alluvium
B
glaciolacustrine silt
basal sand
1 m
paleo-Clark
Fork alluvium
C
F
167503
167501
E
167516
JD-02
167502
167521
A
167520
D
200 cm
167501
180 cm
E
167503
300 cm
260 cm
F
167511
900 cm
167522
850 cm
G
167511
167522
G
167505
167504
167518
167527
H

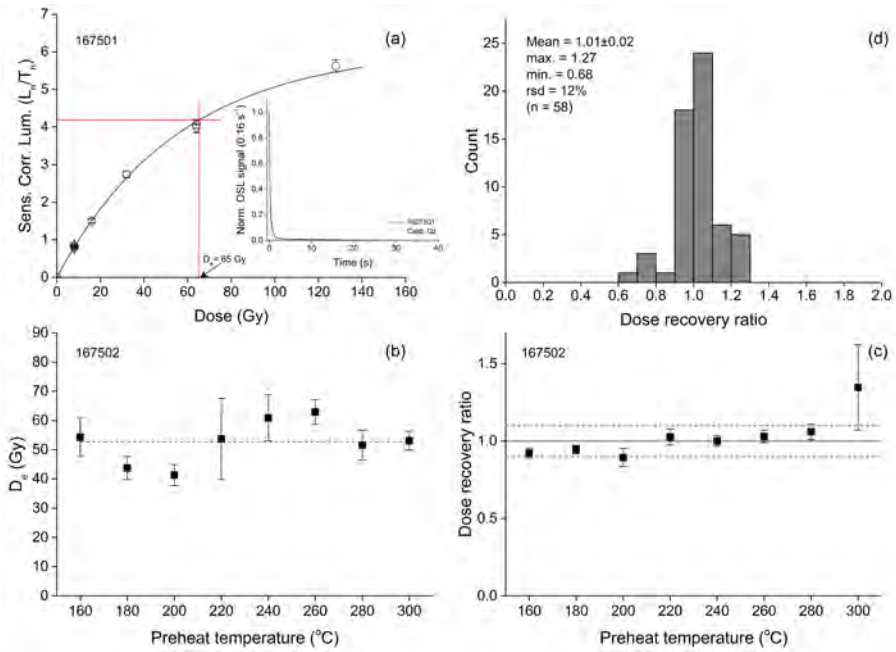
167501
(a)
Sens. Corr. Lum. (L_x/T_x)
Dose (Gy)
D_e = 65 Gy
Norm. OSL signal (0.16 s^{-1})
Time (s)
(d)
Mean = 1.01±0.02
max. = 1.27
min. = 0.68
rsd = 12%
(n = 58)
Count
Dose recovery ratio
167502
(b)
D_e (Gy)
Preheat temperature (°C)
167502
(c)
Dose recovery ratio
Preheat temperature (°C)

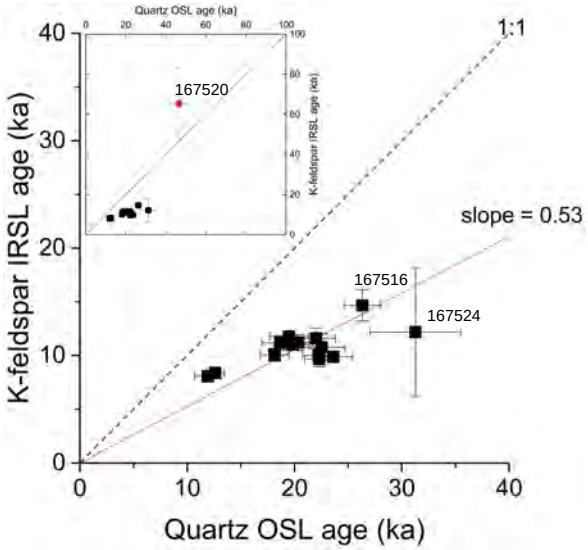
Quartz OSL age (ka)
K-feldspar IRSL age (ka)
1:1
slope = 0.53
167520
167516
167524
0
10
20
30
40

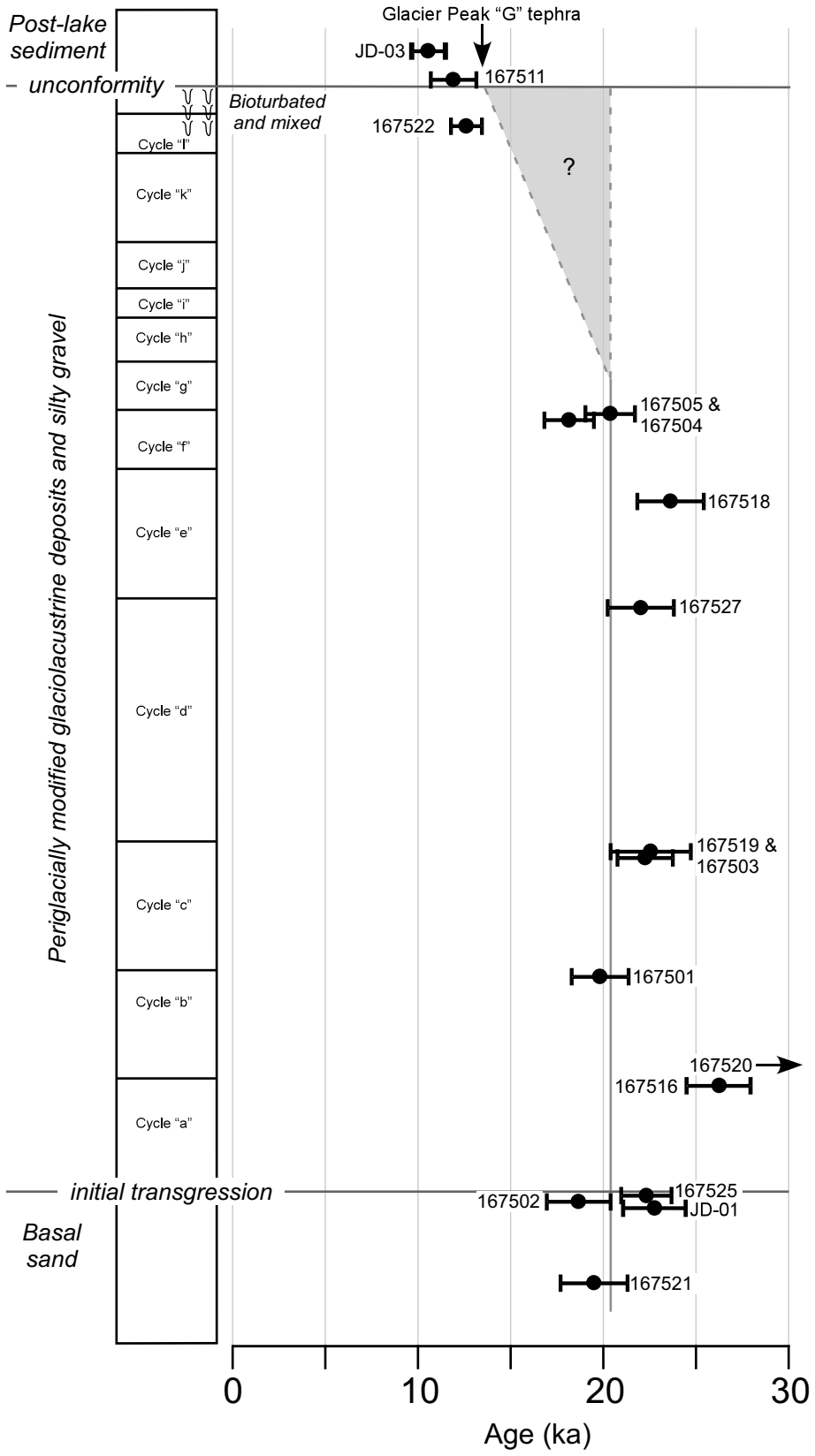
Post-lake sediment
unconformity
Bioturbated and mixed
Glacier Peak "G" tephra
JD-03
167511
167522
?
Cycle "l"
Cycle "k"
Cycle "j"
Cycle "i"
Cycle "h"
Cycle "g"
Cycle "f"
Cycle "e"
Cycle "d"
Cycle "c"
Cycle "b"
Cycle "a"
Periglacially modified glaciolacustrine deposits and silty gravel
167505 &
167504
167518
167527
167519 &
167503
167501
167520
167516
initial transgression
167525
167502
JD-01
Basal sand
167521
0
10
20
30
Age (ka)

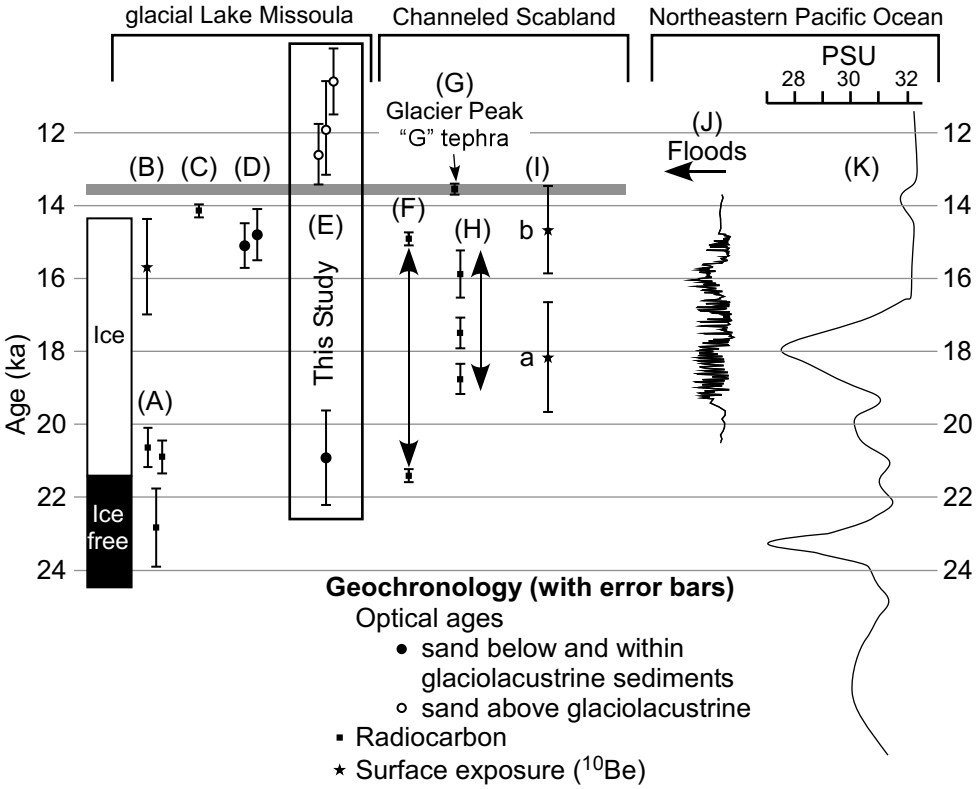
glacial Lake Missoula
Channeled Scabland
Northeastern Pacific Ocean
PSU
28
30
32
(G)
Glacier Peak
"G" tephra
(J)
Floods
(K)
(B)
(C)
(D)
(E)
(F)
(H)
(I)
b
a
(A)
Ice
Ice free
This Study
Age (ka)
12
14
16
18
20
22
24
Geochronology (with error bars)
Optical ages
sand below and within glaciolacustrine sediments
sand above glaciolacustrine
Radiocarbon
Surface exposure (^{10}Be)